INDONESIAN JOURNAL OF SOCIAL AND ENVIRONMENTAL ISSUES (IJSEI)
Journal Homepage: https://ojs.literacyinstitute.org/index.php/ijsei
ISSN: 2722-1369 (Online)
Research Article

Volume 6	Issue 1	April (2025)	DOI: 10.47540/ijsei.v6i1.1615	Page: 94 – 111

Investigating Sediment Grain Size Distribution and Transport Patterns in Punatsangchhu River, Punakha, Bhutan

Sangay Tenzin[1], Ugyen Dorji[1]
[1]Department of Forest Science, College of Natural Resources, Bhutan
Corresponding Author: Sangay Tenzin; Email: samgaytenzin727@gmail.com

ARTICLE INFO

Keywords: Bed Load; Deposition; Erosion; Sediment.

Received : 22 August 2024
Revised : 12 November 2024
Accepted : 29 April 2025

ABSTRACT

This study investigates bed load sediment transport dynamics in selected areas of Punatsangchhu River, focusing on rock type identification, their association with topography, grain size distribution, and factors influencing bed load transport rates. 1D numerical sediment transport modeling was also done in HEC-RAS 6.3.1 using the discharge data of four years from 2020 to 2023. Bed load sediment samples were collected from 55 plots laid systematically 500 meters apart along the river. Results reveal Granite as the predominant rock type, reflecting the region's geological complexity shaped by Himalayan tectonics. Significant associations between rock types and topography, particularly for Granite Boulder, highlight the complex interplay of topographic factors shaping sediment distribution. Bed load transport rates vary across sediment roundness and river reach types, with round particles exhibiting higher rates and riffles displaying greater transport than pools. Regression analysis confirms the significant influence of river velocity and bed slope on transport rates, emphasizing the importance of hydraulic factors in sediment transport processes. The output from HEC-RAS revealed the highest sediment concentration in this valley during the late summer months directly aligning with the higher flow in these seasons. During these years, critical bed changes in some of the cross-sections were also observed. RS 12521 has witnessed the highest deposition rate of about 2.5 meters and similarly, RS 7006 has witnessed the highest erosion rate of about 2.3 meters. Likewise, the profile plot of the river reveals a series of erosion and deposition processes during this time window, affecting the riverbed and consequently channel morphology.

INTRODUCTION

Sediment is a naturally occurring material that is broken down by processes of weathering and erosion, and is subsequently transported by the action of wind, water, or ice (Bogs & Sam, 2006). Sedimentation is a process whereby soil particles are eroded and transported by flowing water or other transporting media and deposited as layers of solid particles in water bodies such as reservoirs and rivers (Tundu et al., 2018). Sediment plays a crucial role in river ecosystems, as it controls the physical habitat of rivers and changes in the amount and distribution of different types of sediment can cause changes in river-channel form and river habitat (Topping, 2020). Sediment comes in all shapes and sizes, from silts and clays to coarse sand and gravel, and each of these kinds of sediment means different things for rivers and aquatic life (Mcclain, 2023).

The sediment supply and transport in the Himalayas is quite significant and is highest in the world (Pradhan, 2004). Bhutan, a landlocked Himalayan nation known for its pristine rivers, faces growing challenges related to sediment transport in its waterways (Palizieux, 2021).The causes of sedimentation in Bhutan's rivers are multifaceted, including climate change impacts, land-use changes, deforestation, and infrastructure development (Simon, 2021). Without effective management strategies, the sedimentation problem is likely to exacerbate, affecting water quality, aquatic habitats, and the efficiency of hydropower generation (Nkonya et al., 2015).

The Punatsang Chhu River, a major river in Bhutan, plays a pivotal role in the region's hydrology, supplying water for irrigation, hydropower generation, and sustaining diverse aquatic species (Choden, 2009). The river's sediment transport pattern is influenced by various factors, including hydrology, climate, geology, land use, and topography (Choden, 2009). The river's sediment transport is complex and dynamic, with a significant portion of the sediment load being transported during the summer months (Shi, 2018).

Rivers in Bhutan have a high development potential for harnessing hydropower because of the mountainous terrain, climatic and other favorable conditions (Tamang, 2004). Despite a program to determine sediment data for Bhutan's rivers no information on sediment transport appears to have been published (DoE, 2003). In spite of many advantages that we get from the natural streams and rivers, the erosion and deposition of sediments in rivers can directly or indirectly lead to many disasters such as floods and failures of hydraulic structures (Thiyagaraja, 2022). HECRAS 6.3.1 (Hydrological Engineering Center's River Analysis System (Vadyman, 2013) version was chosen for modeling the sediment transport in Punatsang Chhu River as this model has been previously used to predict GLOF hazard assessment in Punatsang Chhu basin (Hagg et al., 2021), it is freely available and has already generated realistic results in other studies (Anacona et al., 2015; Satar et al, 2020).

MATERIALS AND METHODS

The study was carried out within Punatsang Chhu river basin. The Punatsang Chhu River has a total length of about 320 km from its source in Bhutan to its confluence point with Brahmaputra in India. Its course in Bhutan has a length of about 250 km (Pradhan, 2008). The two main tributaries, Pho Chhu and Mo Chhu combines at Punakha (27.5921° N, 89.8797° E,), flows from Wangdue (27.4879° N, 89.8996° E) and finally through Tsirang (27.0322° N, 90.1870° E) Dzongkhag before exiting Bhutan to join Brahmaputra in India (Tashi et al., 2022). It is the largest river basin in the country with an area of 9,645 km2 and represents 25% of the country's total land area (MoE, 2003 as cited in Choden, 2009).

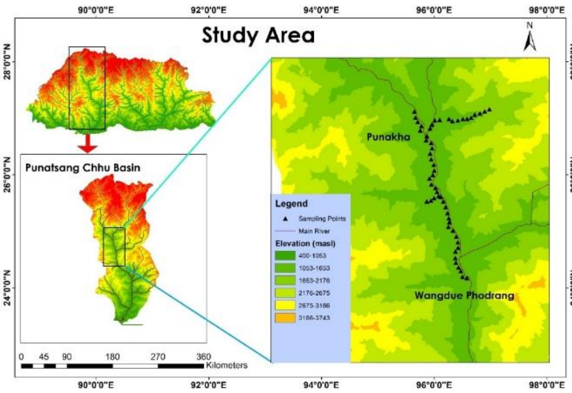

Figure 1. Study Area along Punatangchhu

Sampling Design

A length of approximately 13.41 km along the river from Zomlingthang to PunatsangChhu-Dang Chhu confluence was selected for sampling of river sediments. Another 20 plots from Pho Chhu and Mo Chhu confluence upstream till Sheyngana lower school were assessed. And finally 7 plots were assessed along Toebrong Chhu. These streams are the main tributaries within Punakha that is contributing to the Punatsang Chhu, in discharge and in sediment transport. It falls under Punakha Dzongkhag with the latitude (27.54645438 °N) and longitude (89.87088416 °E). The method of sampling used was systematic random sampling. Sampling site of 13.41 km was further divided into 55 plots of 500 meters apart.

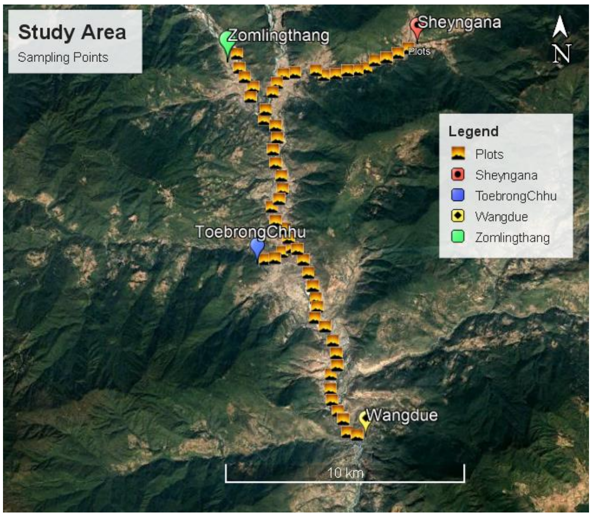

Figure 2. Sampling design showing the location of sampling points.

River sediment data collection: For more efficient and authentic sediment data, sediment samples for each plot was collected from both sides of the river as collection of samples from the middle of the river is practically not feasible to due to the lack of equipment and resources. According to Robert and Christopher (2001), “If bathymetric information is not available, samples from free-flowing rivers or streams should be collected from: Both banks of a relatively straight section of a stream or, on the inside edges of a meander”. Usually, the data collection for river sediments is done in two categories: bed load sediment and suspended load sediment. However, for this study, only bed load sampling was done.

Bed load sediment sampling: In this sampling method, sediment that moves along the bed of a stream by rolling or sliding, called bed load sediment is taken for analysis (Awal et al., 2019). This method is normally used where the sediment movement and velocity of water is close to the bed (Travaglio, 1980 as cited in Awal et al., 2019). A scoop was used for collecting bed load sediment since it can be used to collect samples of every type of sediment. Attaching the scoop to telescoping poles allows for collection of sediments in deeper waters (Robert and Christopher, 2001). Exactly at the plot, 2 meters each from the plot centre was measured, and three samples were collected from each point of 2 meters in length and a composite sample of approximately 1 kilogram was prepared by mixing thoroughly. The depth of water from where the samples were scooped are also recorded using a stick with a graduated scale of 150 meters. And for consistency, bed load sampling was done by one person throughout the area.

River discharge data: The river velocity was determined by using Velocity Probe at sampling point following the guidelines by Global Water (Global Water Flow Probe FP111 Manual.Pdf, 2009). Like sediment sampling, the three consecutive readings from each point were averaged and the mean value was taken as the final reading for the water velocity.

The depth of the river at sampling point were measured using a stick that has the graduated scale in centimeters. However, the river width couldn’t be measured for the PunatsangChhu River and the accurate measurements for river width could only be done at streams (Sheyngana and Toebrong Chhu). River width measurements were estimated among field members, and the approximate reading was then taken.

Similarly, the data on sediment roundness were recorded as (Round, Not Round and Moderately Round) and rive reach types as (Pool, Riffle, Cascade, and Run) as in Yager et al. (2012). Other data like site condition, water temperature, presence of visible pollutants, geo-coordinates, topography features and the specific structures like settlements, bridges, confluence and dredging sites were also recorded.

Lab Analysis

Rock Identification: The samples collected from 55 plots were taken to the lab and dried at room temperature for 24 hours, for grain size analysis. In each sample the different rocks present were identified using a mobile application called ‘Rock Identifier’. Furthermore, the final confirmation of rock types was done consulting an expert

Grain Size Distribution: For this investigation, 800 grams of dried sample from each plot were measured manually and it is sieved using five different sizes of sieve viz. 0.1 mm, 0.2 mm, 0.50 mm, 1 mm, 2 mm and > 2mm (Gale, 2021). . The weights of sediments retained on each sieve were recorded accordingly and the cumulative weights and total cumulative percent of each classes were calculated from these weights. Using sieves of different sizes from fine to coarse allows for the thorough examination of sediment characteristics (Bunte and Steven, 2001), where these sediments can be classified based on sizes.

Bedload Transport Calculation

The sediment transport calculations for this includes the measure of bed load transport and there are wide range of formula available for calculation. From these one of the widely used and most reliable formulae for the bed load transport rate calculation is Meyer-Peter Formula. It is widely used and most reliable for calculating the gravel bed rivers (Kuriqi 2020), whereby the bed material is not just of one size but consists of different ranges of sizes. It can be calculated easily manually and also online. The San Diego State University has the portal developed in their website, where anyone can just feed the data and the bed load transport rate is calculated. The formula is shown below.

$$q_S = \left(39.25 q_{2/3} S_0 - 9.95 d_{50}\right)^{3/2}$$

Whereby, (q) is the flow rate, (So) is the slope of the bed, and (d {50}) is the median grain size of the bed material. The units of the formula are in

U.S. customary units. This formula is mainly used in terms of calculating the bed load transport rate.

The flow rate (q), water velocity was collected from the field using Velocity Probe. A velocity probe, or current meter, is a device used to measure the speed and direction of water flow, specifically in rivers and streams, according to the World Meteorological Organization (WMO). From each plot, three consecutive readings were taken, and the average of the combined reading was taken as the final value. Median grain size (d) is the median size of the sample. The minimum grain size for the calculation of bed load transport must be 3 mm for this formula.

Slope (S) of the riverbed is calculated through ArcGIS (Dolan, 2012). The points recording elevations and the distance of each plot were recorded in SW Ma during field data collection. These points were analyzed using 'Extract Values to Points" tool in ArcGIS. The slope from each riverbed in each plot were then calculated, by dividing the change in elevation by change in the distance between two plots.

Sediment Transport Modelling using HEC-RAS: To accurately model 1D sediment transport in HEC-RAS, DEM of the study area, river discharge, river depth, sediment data and temperature were used. This 1D hydrodynamic model was used to generate water surface profiles, riverbed changes through deposition and erosion and sediment concentration. Quasi-unsteady flow simulation was used to run sediment transport model as in (Rahman et al., 2022). Prior to running the model three categories of data were prepared: geometric data, quasi-unsteady flow file and sediment data.

To create geometric data, DEM with a resolution of 30m x 30m was used, which was obtained from Shuttle Radar Topography Mission (SRTM). The terrain was then added to the RAS mapper, GIS extension in HEC-RAS. The different geometric features of river like river line, bank lines, flow paths and cross-sections were manually drawn using the Google Satellite Map as the reference background layer. It was then exported to HEC-RAS and created as geometric data as shown below.

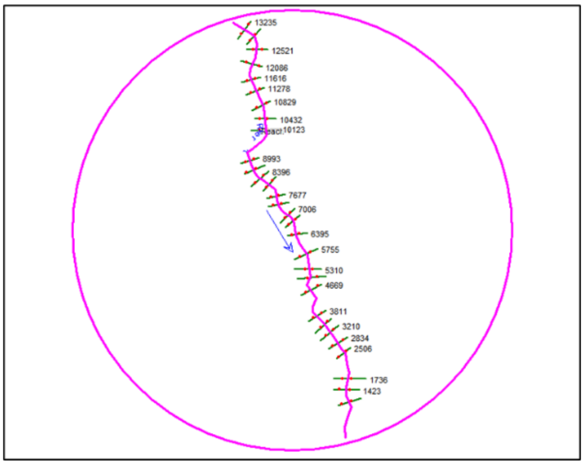

Figure 3. Geometric data of Study River showing river line and cross-sections (RS)

The channel roughness (Manning's coefficient or n-value) was considered from GLOF modelling that typically range from 0.03 to 0.15 (Hagg et al., 2021) where channels are found usually rough in Himalayas. Rahman et al 2022, considered Manning's roughness coefficient for sediment transport modelling from 0.034 to 0.195, however directly adapting the coefficient value from completely different geographical areas cannot give realistic results. According to HEC-RAS n-values between 0.025 and 0.075 are typical (Bruner et al., 2016). Therefore, considering all these scenarios Manning's value adapted for this study was 0.05 to 0.14 whereby (0.05 = smooth, 0.10 = medium and 0.14 = rough).

In sediment data, the boundary conditions used was Rating Curve in sediment load series (Rahman et al., 2022) as shown below in (fig. 3.4). The initial conditions and transport parameters was based on the maximum river depth that is 5m from the field observation. And the bed gradation sample was created from the sieve analysis in five classes (VFS = Very Fine Sand, FS = Fine Sand, MS = Medium sand, CS = Coarse Sand and VCS = Very Coarse Sand). These sizes in mm were plotted against % finer, which is an average cumulative percent weight of each of those grain classes.

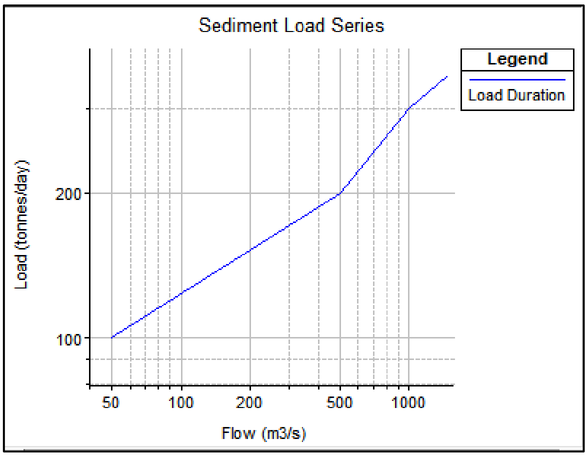

Figure 4. (a). Rating Curve plotted against load (tons/day) and flow (m^3/s).

The sediment transport function used for the computation of the transport model was Laursen (Copeland) method (Equation 1), (Mohamed et al., 2018). And the sorting method is also Copeland (Ex7) for this transport function. Similarly, the Fall Velocity method used was Rubey Method (Molinas and Wu, 2001) shown in equation 2.

$$C_m = 0.01\gamma \left(\frac{d_s}{\pi}\right)^{\frac{7}{6}} \left(\frac{\tau_0'}{\tau_w} - 1\right) f\left(\frac{u_0}{\omega}\right) \text{-- equation 1}$$

Whereby,

C_m = concentration of the sediment discharged (tones/day)

γ = unit weight of the water

d_s = Mean particle diameter

D = mean particle diameter

τ_0' = bed shear stress due to grain resistance

τ_w = critical bed shear stress

ω = particle fall velocity (m/s)

$$\omega = F_1\sqrt{(s-1)gd}$$

$$F_1 = \sqrt{\frac{2}{3} + \frac{36v^2}{gd^3[s-1]}} - \sqrt{\frac{36v^2}{g\,d^3[s-1]}} \text{ --- equation 2}$$

Whereby,
v = Kinematic viscosity
s = Specific gravity of particles
d = Particle diameter
g = Gravitational acceleration (m/s^2)

The Laursen (Copeland) method in transport function can predict the total sediment load. This method is applicable for the sediment grain size of 0.011 to 29 mm (Hamzah, 2014). Therefore, it is found feasible to be used for this model.

Results and Discussion

Types of Sediments and Grain Size Distribution

Identification of River Sediments: The rocks identified are Granite, Granite Boulder, Gneiss, Gneiss Boulder, Dark Gneiss, Quartzite and Schist. The occurrence of these rocks in terms of frequency and the cumulative Percent is shown below.

Table 1. Frequency table for rocks whereby 0 for absence and 1 for presence.

Rocks		Frequency	Percent	Cumulative Percent (100%)
Granite	0	11	20.0	2.85
	1	44	80.0	11.4
	Total	55	100.0	-
Quartzite	0	33	60.0	8.57
	1	22	40.0	5.71
	Total	55	100.0	-
Granite Boulder	0	35	63.6	9.08
	1	20	36.4	5.20
	Total	55	100.0	-
Gneiss	0	32	58.2	8.31
	1	23	41.8	5.97
	Total	55	100.0	-
Dark Gneiss	0	17	30.9	4.41
	1	38	69.1	9.87
	Total	55	100.0	-
Gneiss Boulder	0	24	43.6	6.22
	1	31	56.4	8.05
	Total	55	100.0	-
Schist	0	16	29.1	4.15
	1	39	70.9	10.12
	Total	55	100.0	-

The Himalayas are generally found to be characterized by the diverse types of rocks such as granitic, gneissic, and schistose metamorphic rocks in the southern part of the Higher Himachal Himalaya (Kakar, 1988), and quartzite, granite, and phyllite boulders in a rugged terrain (Ansari, 2013). The most dominant rock occurring within this area is Granite, followed by Schist and Dark Gneiss, whereas the least occurrence is shown by Granite Boulder. This may be attributed to the Granite's wide range of sources which have a significant correlation to tectonic settings of the Himalayas (Pearce, 1996).

Occurrence of Rocks With Topography

Each of the 55 plots were classified into five different topography classes (Flat, Valley, Sloped, Confluence, Hilly) based on observation following (Duta & Maha 2024). Therefore, in order to draw the relation of the occurrence of these rock types in terms of different topography, a chi-square test in SPSS 26 was performed.

Table 2. Chi-square test results showing different significance value for the association between rock types and topography.

Rock types	Asymp.sig. (2-sided)
Granite	$P>0.05$
Quartzite	$P>0.05$
Granite boulder	$P<0.05$
Gneiss	$P>0.05$
Dark Gneiss	$P>0.05$
Gneiss Boulder	$P<0.05$
Schist	$P>0.05$

The chi-square test revealed a statistically significant association between Granite Boulder and topography ($p<0.05$). This suggests that the occurrence of Granite Boulder varies significantly across different topographic features along the Punatsang Chhu River. However, no significant associations were found between other rock types (Granite, Quartzite, Gneiss, Dark Gneiss, Gneiss Boulder, and Schist) and topography ($p>0.05$). This indicates that the distribution of these rock types remains consistent across different topographic settings.

The significant association observed for Granite Boulder suggests that its occurrence may be influenced by specific topographic characteristics, such as slope gradients or depositional environments.

The relation of rocks with topography is a complex phenomenon which is induced by many factors (Guidmond et al, 2022) and the reason for not showing any significant association with the topography in this case can be due to almost similar topography type. Moreover, the study site is stretched along the Punakha and Wangdue valley which does not show any significant variations in topography. According to (Korup, 2008), the occurrence of different rock types is closely related to topography, with distinct topographic signatures being associated with specific rock types. The different features of landscapes undergo different changes.

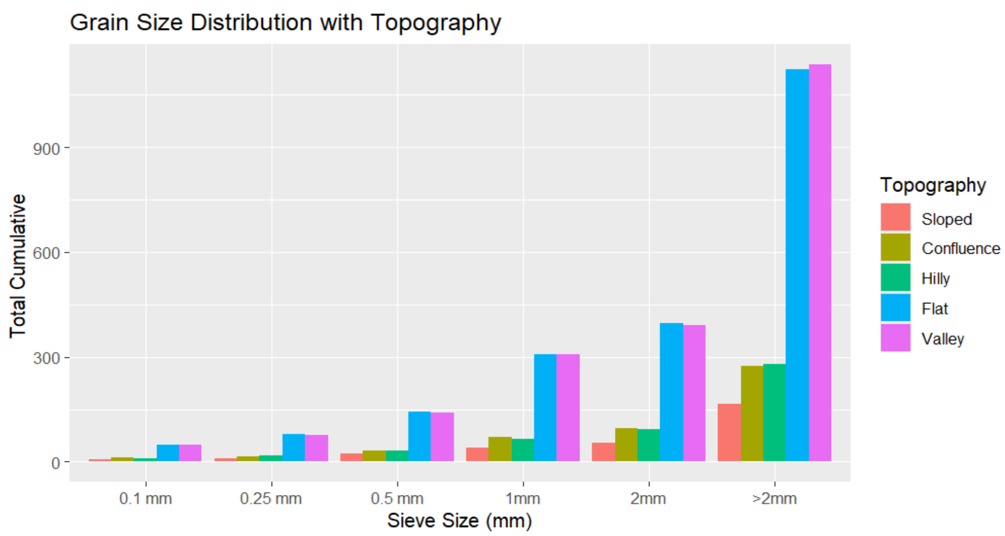

Figure 5. Grain size distribution with topography types plotted as sieve size against total cumulative

Due to varying conditions of climatic and geological settings which can ultimately affect the formation and transformation of rocks including weathering (Mibei, 2014).

Grain Size Distribution

From the graph, the sediment grain sizes of more than 2 mm has the highest distribution in all the topography types and grain size of 0.1 mm has the minimum distribution across different topography types. From those topography types the flat and valley areas have higher distribution and the slopes and confluence have the lowest distribution of sediment grain size.

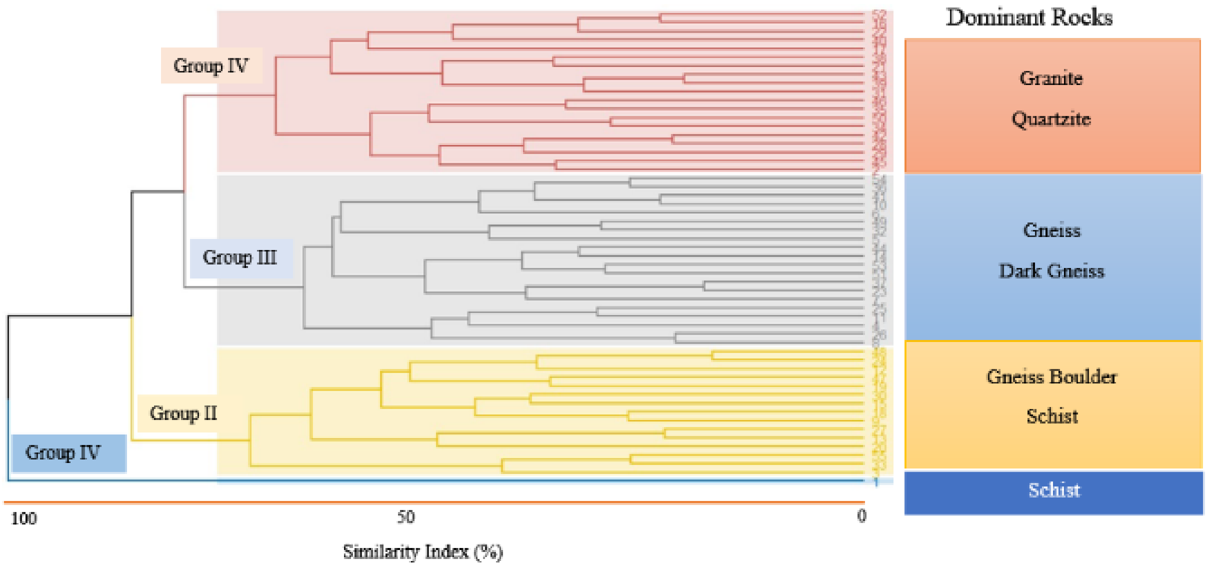

Figure 6. Dendrogram showing the grouping of similar plots

The hierarchical clustering of rock types and grain size distribution across 55 plots revealed 4 distinct groups of similar plots with similar rock compositions. These clusters don't necessarily limit to only those specified rock types, as the presence of other rock types were also observed. Nevertheless, the dominant rock types occurring in these groups were used to identify clusters. These structures indirectly relate to the rock compositions and grain size distribution within a cluster.

Calculation of Bed Load Transport Rate

The sediment transport rate is calculated using Meyer-Peter Formula as shown below.

$$q_S = \left(39.25 q_{2/3} S_0 - 9.95 d_{50}\right)^{3/2}$$

Whereby, (q) is the flow rate, (So) is the slope of the bed, and (d {50}) is the median grain size of the bed material. The units of the formula are in U.S. customary units. This formula is mainly used in terms of calculating the bed load transport rate. The descriptive statistics shown below present minimum and maximum sediment transport rate along with the mean transport rate, all in units, kg/s/m.

Table 3. Descriptive statistics of sediment transport rate

	N	Minimum	Maximum	Mean
Rate(kg/s/m)	55	23.19	133.33	62.01

Bed Load Transport Rate with Sediment Roundness and River Reach

Table 4. Number of different types of sediment roundness and reach sampled.

	Type	N
Reach	Cascade	20
	Run	34
	Riffle	1
	Total	55
Sediment Roundness	Moderately Round	12
	Round	38
	Not Round	5
	Total	55

Bedload Transport Rate with Sediment Roundness

The Kruskal-Wallis test was conducted to examine the distribution of bed load transport rates among different sediment roundness types (Round, Not Round, and Moderately Round). A total of 55 samples were included in the analysis. The test yielded a significant result ($H(2) = 34.614$, p <

0.001), indicating that the bed load transport rate varied significantly across the different sediment roundness categories. Subsequent pair-wise comparisons using adjusted Bonferroni correction revealed significant differences in bed load transport rates between Round and Not Round ($p < 0.001$), Round and Moderately Round ($p < 0.001$), but not between Not Round and Moderately Round ($p = 0.167$). These findings suggest that sediment roundness has a significant effect on bed load transport rates.

The difference in bed load transport rates between round, not round (angular), and moderately round sediment particles is primarily due to their shapes and how they interact with fluid flow (Khosravi, 2020). Round particles, with smooth, streamlined shapes, experience less resistance to flow and are easily transported downstream (Cassel, 2021). Not round or angular particles have irregular shapes that interlock, resisting movement and resulting in lower transport rates compared to round particles. Moderately round particles fall between round and angular shapes, showing higher transport rates than angular particles but lower rates than truly round particles due to their intermediate resistance to flow (Durafour et al., 2015).

Round particles, characterized by high circularity indices, feature smooth and symmetrical shapes that minimize resistance to flow, facilitating easy entrainment and transport even at lower current flow velocities. Conversely, non-round or angular particles exhibit rougher surfaces and asymmetrical shapes, increasing resistance to flow and making them more challenging to transport compared to round particles. Moderately round particles, falling between these extremes, demonstrate intermediate bed load transport rates due to their partially smooth yet not perfectly symmetrical shapes, resulting in an intermediate resistance to flow (Durafour et al., 2013).

Bedload Transport Rate with River Reach

Similarly, the Kruskal-Walli's test was conducted to examine the distribution of bed load transport rates among different river reach types (Pool, Riffle, Run and Cascade). A total of 55 samples were included in the analysis. The test resulted a significant result ($H(3) = 47.039$, $p < 0.001$), indicating that the bed load transport rate varied significantly across the different river reach types. Subsequent pair-wise comparisons using adjusted Bonferroni correction revealed significant differences in bed load transport rates between Pool and Run ($p < 0.05$), Pool and Riffle ($p < 0.001$), Cascade and Riffle ($p < 0.05$) and Cascade and Run ($p < 0.001$). However, no significant differences in bed load transport rate were observed between Pool and Cascade ($p = 0.710$) and Run and Riffle ($p = 0.096$).

The bed load transport rates differ between pools and riffle within the river reach. Generally, riffles exhibit higher sediment transport rates compared to pools. At the riffle head and pool centre, sediment transport rates are typically higher, while the riffle tail tends to have lower rates (Hassan et al., 2022). This difference is highlighted by the observation that Sediment transport rates are greater upstream of riffles compared to downstream. During storm events, transport rates remain higher at the upstream riffle. Conversely, during smaller flow events, sediment tends to accumulate in pools, resulting in lower transport rates compared to riffles (Estep and Beschta, 1985).

River Reach and Sediment Roundness

To point out any underlying relations of river reach types with different shapes of sediments, Chi-square test was performed.

Table 5. Cross-tabulation of sediment roundness types and river reach types.

		Sediment Roundness			Total
		Moderately Round	Not Round	Round	
River Reach	Cascade	22	0	1	23
	Pool	1	3	0	4
	Riffle	0	0	15	15
	Run	9	0	4	13
Total		32	3	20	55

Further interpreting the plot, it shows the concentration of sediment in all these years was seen highest in the July and August month. The Highest concentration of sediment recorded at this station was 8.5mg/l, and the lowest concentration of sediment recorded at this station was close 0.1mg/l.

The chi-square test was conducted to examine the relationship between sediment roundness and river reach types. Both Pearson Chi-Square and Likelihood Ratio tests yielded significant results, with values of $\chi^2(6) = 78.311$, $p < 0.001$ and $\chi^2(6) = 63.805$, $p < 0.001$, respectively. A total of 55 valid cases were included in the analysis.

The significant results indicate a strong association between the different types of sediment roundness and river reach types. Specifically, riffle sediments were found to be coarser and better sorted compared to pool sediments, reflecting the reversal of bottom velocity/shear stress hierarchy between pools and riffles at high flow. Additionally, riffle sediments were observed to be less spherical than pool sediments, with shape differences primarily dependent on size (Hirsch & Abrahams, 1981). Runs, serving as transitional zones between pools and riffles, typically contain a mixture of rounded and moderately round particles, facilitated by moderate flow velocities (Montgomery and Buffington, 1997). Cascades, characterized by turbulent flow oversteps or ledges, were found to facilitate intense sediment transport, including both rounded and angular particles of various sizes and shapes (Schumm, 1960).

Bed Load Transport Rate with the River Velocity

In order, to understand the effect of river velocity with the bed load transport rate regression analysis was conducted. The test showed a strong and statistically significant positive association with bed load transport rate ($B = 142.224$, $SE = 7.308$, $\beta = .937$, $t = 19.461$, $p < .001$) which indicates that for each m/s increase in river velocity, the predicted bed load transport rate increases by 142.224 kg/m/s.

Initial rapid increase in bed load transport observed with seepage suggests a positive correlation between flow velocity and sediment entrainment. This relationship conforms to the conventional understanding that elevated flow velocities induce greater shear stress on the channel bed, thereby facilitating the mobilization and transportation of sediment particles (Sharma et al., 2019). Bed load transport fluctuations decrease with higher river velocities, especially during rising flow conditions, indicating a direct positive correlation between river velocity and bed load transport rate in sediment transport dynamics (Rickenmann, 2023).

As the velocity of the river increases, there is a corresponding rise in the rate of bed load transport due to improved effectiveness in sediment movement (Cassel et al., 2021). This escalation in river velocity results in a greater force exerted by the flowing water on sediment particles. Consequently, this heightened force enables the river to pick up and carry more sediment particles along its bed (Gomez and Soar, 2022).

Bed Load Transport Rate with Slope

Similarly, regression analysis was performed between the bed load transport rates and the riverbed slope. The tests showed a strong positive and statistically significant association with ($B = 31.698$, $SE = 2.743$, $\beta = 0.864$, $t = 11.556$ and $p < 0.001$) which suggests that with each degree increase in slope, the bed load transport rate increases by 31.698 Kg/m/s.

The slope of the riverbed significantly affects the bed load transport rate. Sekine & Parker (1992) found that the ratio of transverse to stream-wise bed-load transport increases with increasing transverse slope. Damgaard et al., (1997) further noted that existing theories for bed load transport on slopes are not adequate for all bed slopes and proposed a semi-empirical relation that predicts the transport rate on different slopes. Rickenmann (1991) observed that bed load transport rates increase with increasing fluid density, particularly when the flow around the grains is not laminar. Recking (2012) highlighted the impact of sediment supply on bed load transport rates, with higher rates in streams connected to an active source.

Bed Load Transport Rate with River Width

Another factor affecting the bed load transport rate is river width or the cross-sectional length of the river. For this, Spearman's correlation test was performed to see how the bed load transport rate is changing with change in river width. A total of 55 samples were included in the analysis. The correlation test was not statistically significant, although there appears to be slight negative monotonic relationship between the bed load transport rates and river width (Spearman's rho = -0.152, one-tailed $p = 0.134$, $N = 55$). Additionally, the correlation coefficient between river width and bed load transport rate was also -0.152, which was not statistically significant (one-tailed $p = 0.134$, $N = 55$).

The relationship between river width and bed load transport is complex and varies depending on the specific conditions. (Warburton, 1996) found that narrower channels tend to have higher bed load transport rates, while Carson and Griffiths (1987) suggested the existence of an optimum width that maximizes capacity. Young (1989) further explored this, noting that bed load transport rate is dependent on channel form and can be more efficient under steady flow. However, Warburton and Davies (1994) found that bed load transport rates vary significantly within a given set of controlling variables, indicating that the relationship between river width and bed load transport rate is not straightforward.

1D Sediment transport modelling using HEC-RAS

The HEC-RAS model was calibrate using the Manning's value. The Manning's value for the left, right and main channel were entered manually. Manning's value used for this study was 0.025 to 0.034 whereby (0.025 = smooth, 0.030 = medium and 0.034 = rough) (Bruner et al., 2016; Hagg et al., 2021).

River discharge data was based on data from NCHM (Wangdi Station) which comprises of daily discharge data for the period of four years from 2020 to October 2023. Other data like sediment, river depth and temperature collected from the field were all combined to simulate the sediment transport.

Sediment Concentration

Figure 7. shown below depicts a sediment concentration at river station RS: 12521. This station was chosen since it was the starting River Station for this model. It also shows how much sediment load in concentration has entered in the study area. The sediment concentration according to the plot below was highest in the year 2020, followed by the year 2023. The year 2021 has the lowest sediment concentration at this station.

Further interpreting the plot, it shows the concentration of sediment in all these years was seen highest in the July and August month. The Highest concentration of sediment recorded at this station was 8.5mg/l, and the lowest concentration of sediment recorded at this station was close 0.1mg/l.

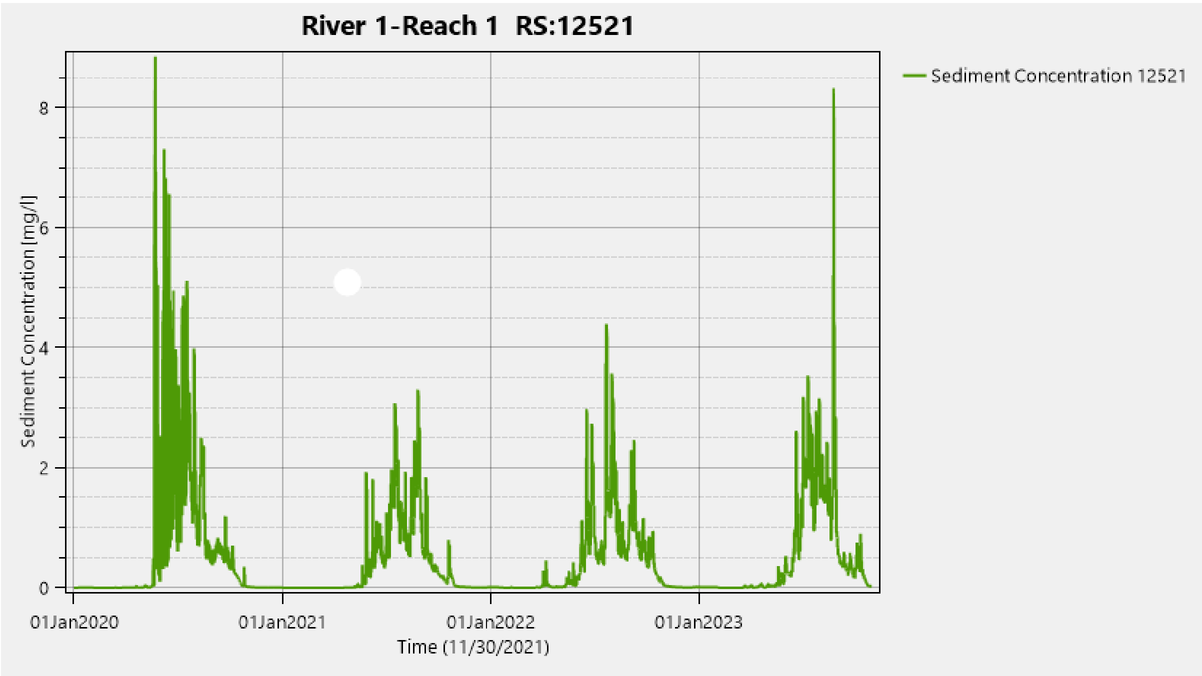

Figure 7. Sediment Concentrations (mg/l) at RS 12521 during 2020 to 2023.

The sediment concentration in the rivers closely relate to the flow conditions, with generally higher concentration during peak flow seasons (Karim and Kennedy, 1987). The higher concentration of sediments in late summer months can be due to the higher flow current which helps in carrying more sediments. It can also be due to rainfall, which helps erode loose soils and particles from adjoining areas into the main river (Zhang et al, 2017). This is in line with the river velocity as one direct factor affecting the total load of sediment transport which is discussed earlier.

Critical Bed Changes (deposition and erosion) Due to Sediment Transportation

After running the sediment transport simulation for time window of almost four years, the cross-section of riverbed were inspected. Some stations showed deposition activities, some stations showed erosion processes and some stations has undergone very minimal change. The cross-section at RS 12521, RS 11616, RS 10432, RS 10123, RS 7677 and RS 6780 showed notable deposition over the past four years. The cross-section change plot of RS12521 and RS 6780 was selected as these two RS(s) showed highest deposition among others.

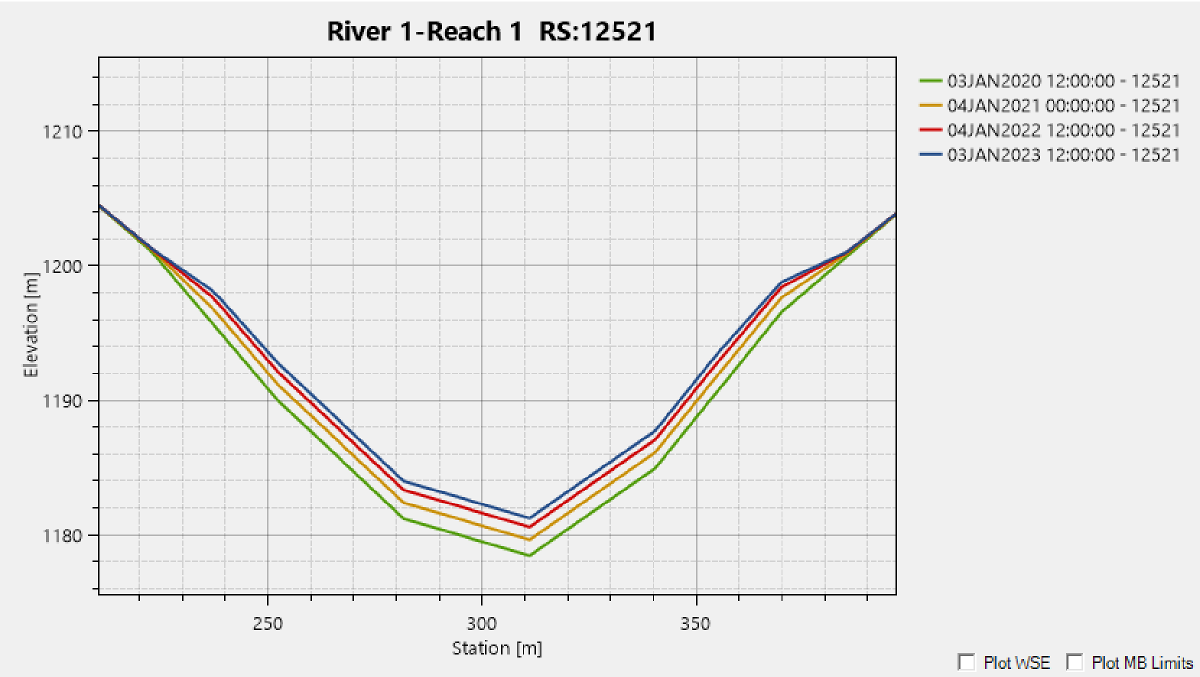

Figure 8. Deposition Highest at RS 12521 during 2020 to 2023.

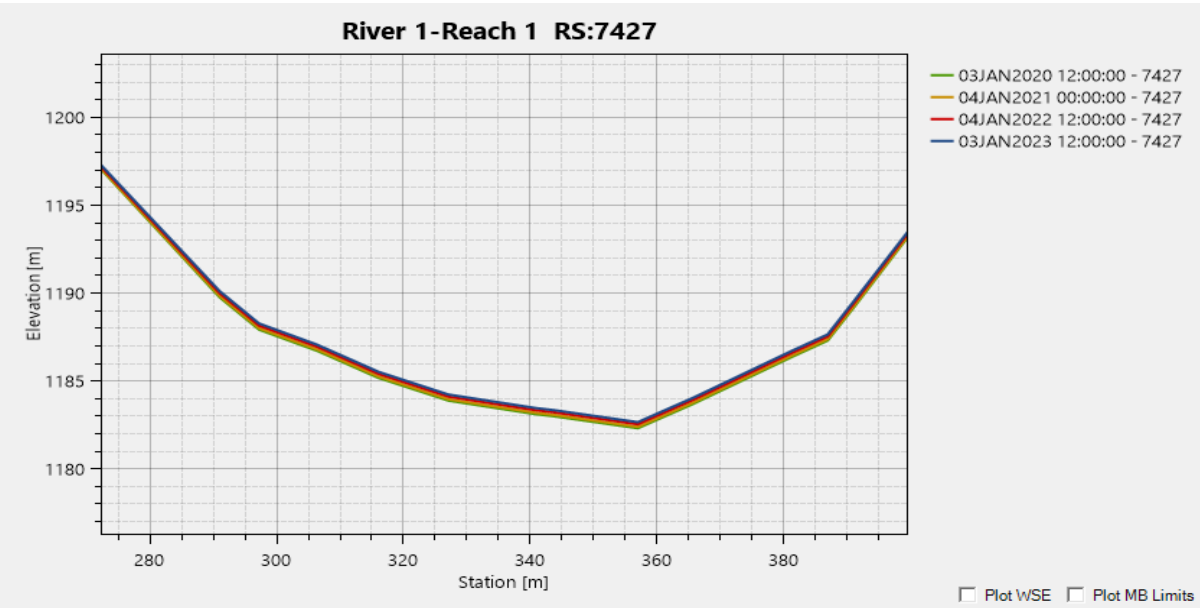

Figure 9. Deposition Lowest at RS 7427 during 2020-2023.

The highest increase of elevation was recorded at RS 12521 of about 2.5m. The figure 8 and figure 9 shows the magnified view of HEC-RAS output showing the change in elevation due to deposition in these stations in different years. The initial elevation level shown by year 2020 with a green color and the final elevation level shown by year 2023 with blue color. The RS 12521 had the highest deposition and RS 7427 had the lowest deposition of about 0.3m.

The deposition pattern of sediments along the river depends on outflow inertia, bed friction and outflow buoyancy (Wright 1977), with higher outflow inertia and buoyancy decreases deposition rates and higher friction of bed increases deposition rates. The highest deposition at this RS may be due to either of these factors. The deposition of sediments occurs usually when the flow decreases and riverbed slope increases. The particles in the absence of shear stress due to the flowing current of river tend to settle down, as when rivers lose energy the particles settle down with larger particles first (Kellerman and Gorelick, 1996).

To the contrary, some of the river bed in few stations have undergone a decrease in elevation. The highest decrease in elevation was seen in RS 7006 (about 2m) and the lowest in RS 8993 (about 0.2m). The 10 figures show the highest erosion and lowest erosion of river bed.

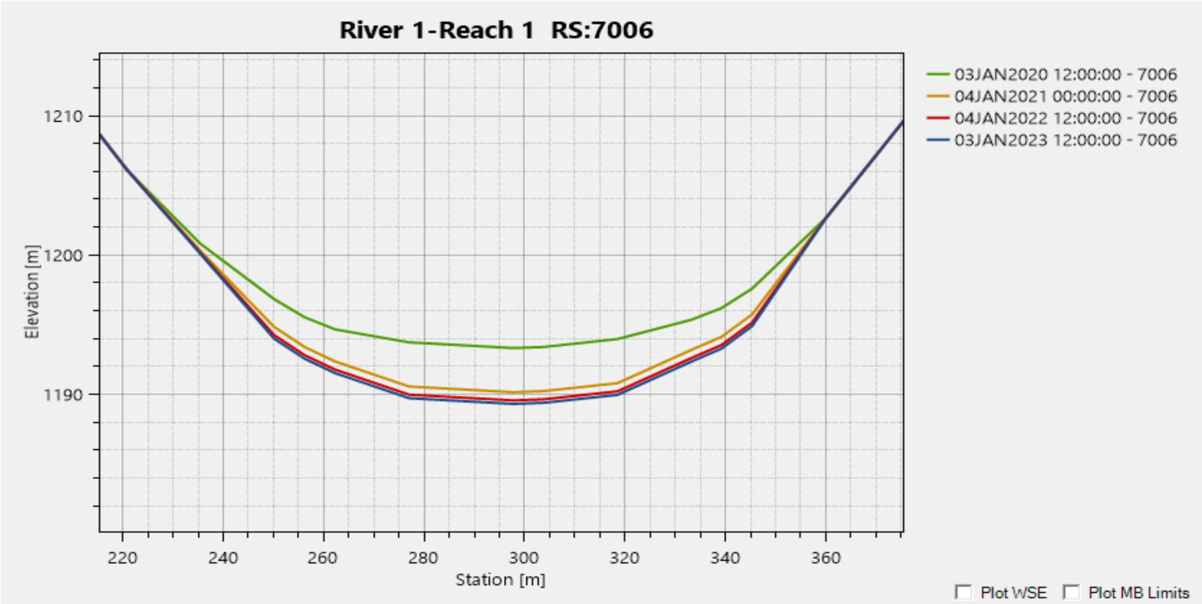

Figure 10. Erosion maximum at RS 7006 during 2020 to 2023.

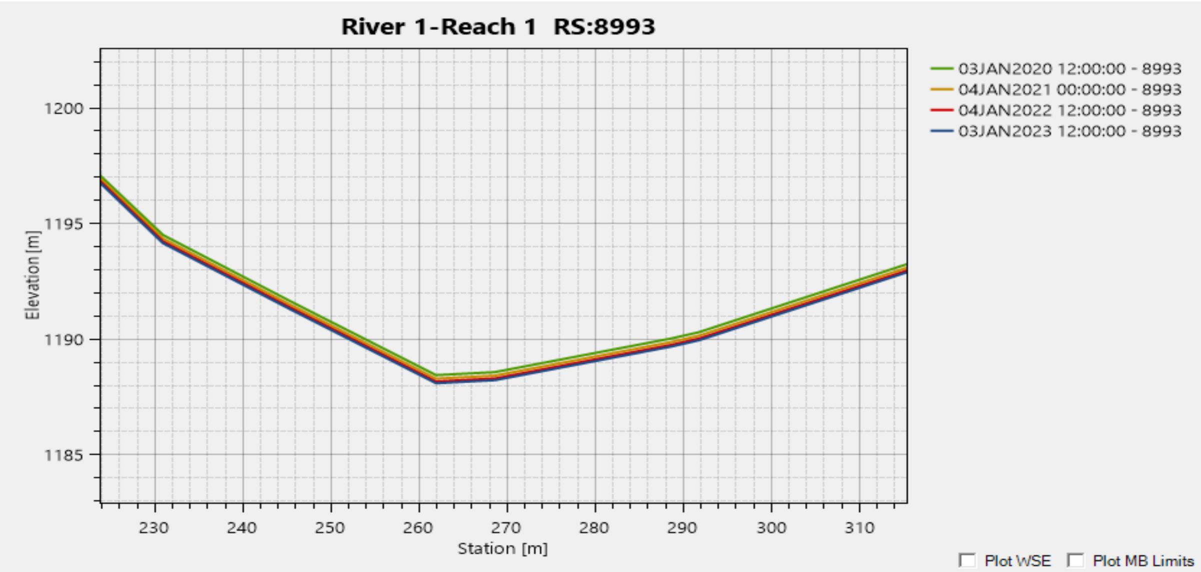

Figure 11. Erosion minimum at RS 8993 during 2020 to 2023.

The erosion of river bed occurs through abrasion and attrition (Galay, 1983) mainly dependent on the flow current and river bed slope. The higher flow in these stations could be the reason for more erosion processes. The erosion rates in the Punatsang Chhu drainage basin vary, with lower rates in the low-relief zone and higher rates in the high-rainfall regions (Portenga, 2015). Stream bed weathering can also enhance the bed erosion by water and debris flow in headwater bedrock channels (Howard, 1998). Howard and Kerby (1983) and Howard (1994) proposed that the arte of bedrock erosion is proportional to the shear stress exerted by runoff, with an implicit assumption that the bedrock can be directly scoured off by run off.

Effective width Changes of River During Different Flow Periods

The river width shrinks and expands in open plains depending on different flow volumes. This change in width was well exhibited at RS 12521. The change of the river maybe attributed to various factors like flow condition, bank stability and flow current. The higher erosion property of the bank can induce the river to expand in plains. The figure shown below shows an effective width change ranging approximately from 50m to 102m, in normal view (Figure 12) and the enlarged view (Figure 13).

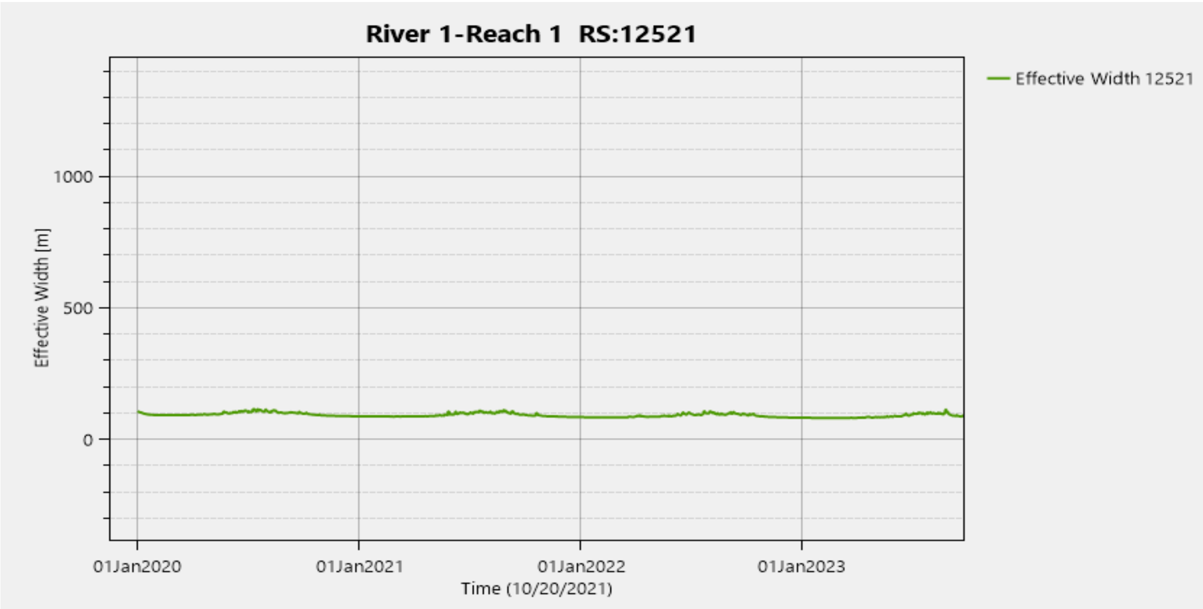

Figure 12. Effective width change at RS 12521 during 2020 to 2023.

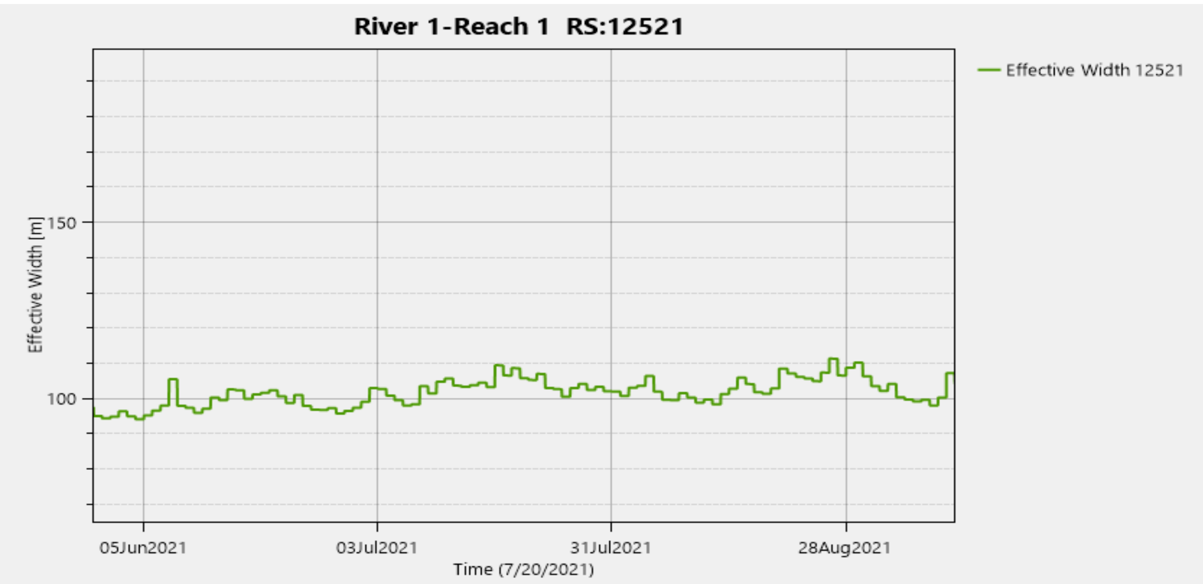

Figure 13. Magnified view of effective width change at RS 12521.

It is showed that at this station the width of river can expand to about 102m during late summer months. The river at plains, basically when the boundary conditions are relatively at same elevation tend to overflow and expand thereby, increasing its effective width. This is a valuable information that can be used for flood inundation mapping as it clearly depicts the areas that river can cover at certain flow scenarios.

The changes in the width of river downstream is also related to the slope and grain size (Pitlick and Cress, 2022) whereby decrease in the slope of the river downstream can lead to increase in the overall width of the river. It is reported that river adjustment have varied causes and in some cases the widening can occur by erosion of one or both banks without substantial incision (Pizzuto, 2013). In many cases of flood mapping and risk planning, the river is a crucial component, and understanding the changes in the river width can aid in better planning of flood hazards.

Overall Changes in River Profile

Figure 14 shows the over change in elevation of river bed throughout the river profile. This gives the overall visualization of various depositions and erosions that has occurred in the, river during the given time window. The green line, indicating initial conditions at year 2020 and the blue line indicating the final conditions at 2023, shows that some sections of the river has undergone erosion while some sections have undergone deposition at certain rates.

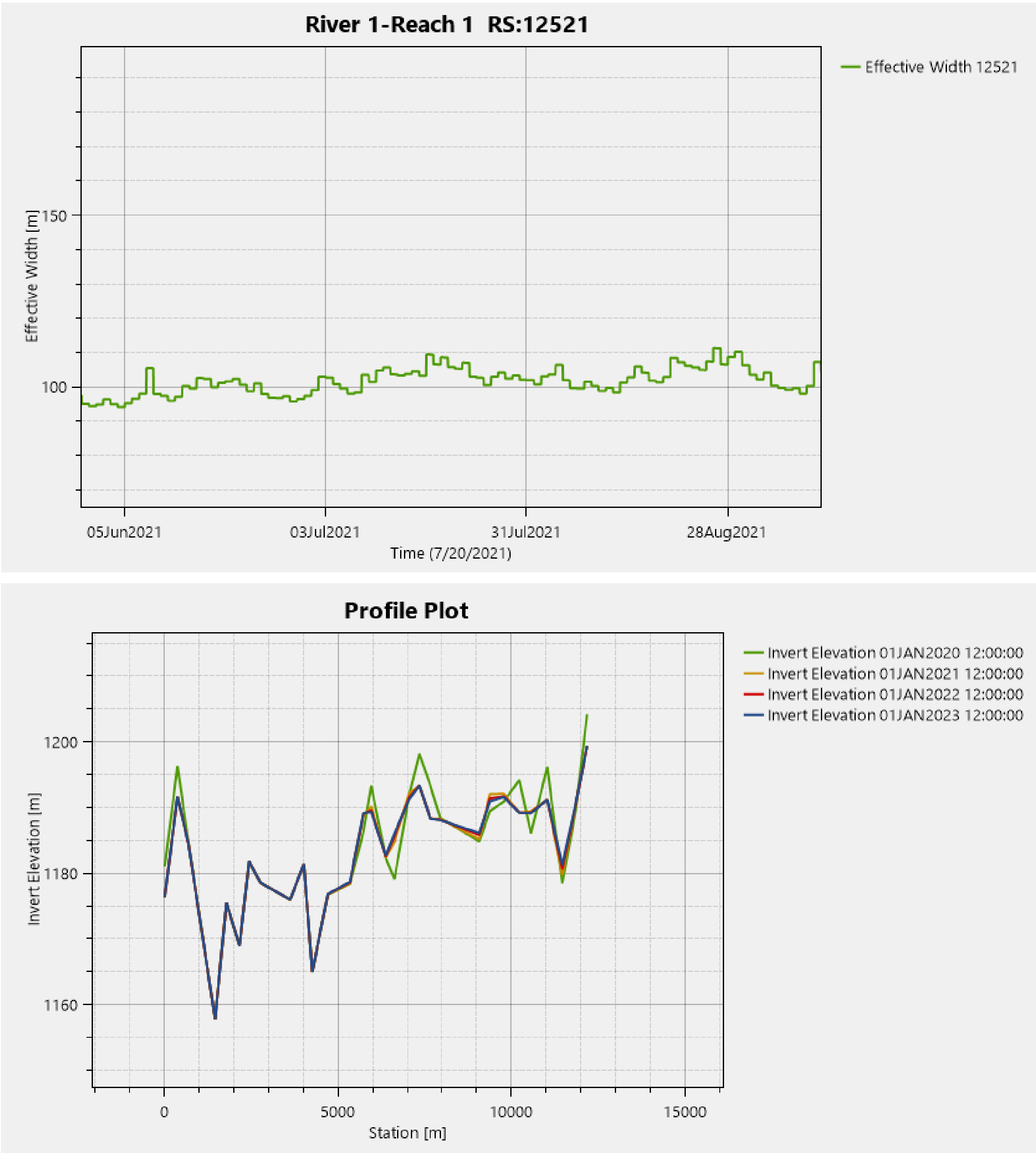

Figure 14. Change in river profile during 2020 to 2023.

However, it is also shown that some section of the river bed in the above profile, has neither undergone deposition nor erosion, or simply the change (erosion and deposition) is very minimal. Changes in channel geometry are determined both by changes in water discharge (Leopold and Maddock, 1953) and by changes in sediment load and bank properties (Schumm, 1960). Large-scale temporal and spatial bed-level changes are generally a result of changes in the occurrence and duration of high and low discharges over several years, the grain size-specific sediment flux or the base level (Gilbert, 1877; Mackin, 1948; Lane, 1955; Blom et al., 2017). Such changes noted in the Punatsang Chhu river over the course of years maybe also due one of these reasons.

Daily Flow for the Period of 2020-2023

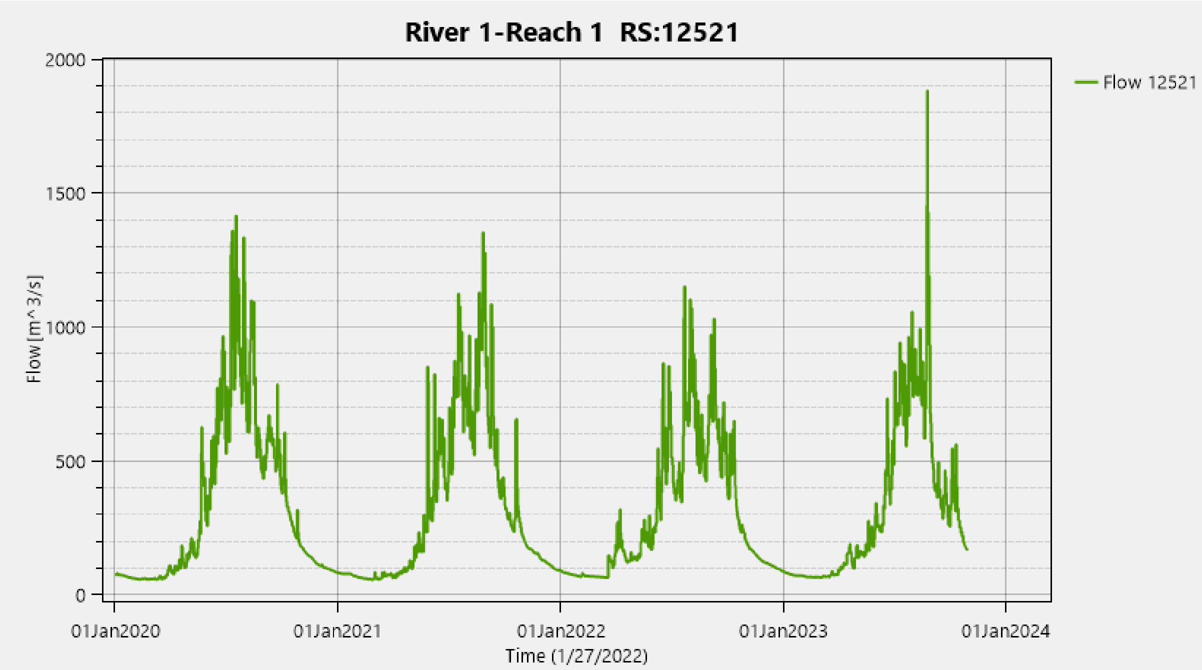

Figure 15. Daily discharge for the period of 2020-2023.

Conclusion

The dominant rock types present along the river are Granite, Granite Boulder, Quartzite, Gneiss, Gneiss Boulder, Dark Gneiss and Schist. Of these rock types the most dominant was Granite with 11.4% of total cumulative percent. Granite Boulder showed statistically significant association with the topography types. Sieve analysis done with five different sizes (0.1mm, 0.25mm, 0.5mm, 1mm, 2mm and >2mm) showed the occurrence of sediments in varying sizes and classes. The grain size distribution graph plotted against topography types revealed higher distribution of sediments of sizes greater than 2mm in all the topography types than the other classes of grain sizes.

The bed load transport rates calculated from the Meyer-Peter formula gave the maximum rate of 133.33 kg/s/m, mean rate of 62.01 kg/s/m and minimum rate of 23.19 kg/s/m. A Chi-square test between the transport rates with sediment roundness and river reach types showed statistically significant association. The round sediments were found to be transported faster and more in the reaches like cascade and run. The riffle sediments were coarser and the round sediments dominate the pools. In terms of river velocity and river bed slope, positive correlation was observed with the bed load transport rate showing an increase in 142.224 kg/m/s with every m/s increase in velocity and increase of 31.698 Kg/m/s for degree increase in the river bed slope. The correlation test between river width with transport rate was not statistically significant, although there appears to be slight negative monotonic relationship between the bed load transport rates and river width (Spearman's rho = -0.152, one-tailed p = 0.134, N = 55). Additionally, the correlation coefficient between river width and bed load transport rate was also -0.152, which was not statistically significant (one-tailed p = 0.134, N = 55).

The integrated monitoring and assessment of sediment transport in this basin is necessary to prevent any sediment related issues along the river. Erosion and deposition trend of the riverbed must be understood well before constructing any hydraulic structures. Understanding erosion and deposition trends is vital before constructing hydraulic structures, as areas like RS 7006 (high erosion) and RS 12521 (high deposition) require targeted engineering solutions such as scour protection and sediment control systems. engineeri Sediment fingerprinting can help identify the possible areas in the upstream areas of river that are contributing to river load. Reforestation, soil conservation practices and better land management in those areas can help reduce erosion thereby reducing the total sediment budget. In the areas where, sediment deposition rates are higher, it is advisable to implement sediment removal activities such as dredging and sediment excavation since these accumulation of sediments in the long run poses risk to infrastructures and ecosystem. It is necessary to develop adaptive management plans that allows for the flexible responses to changing conditions and mitigate the negative impacts of sediment transport in rivers, to better promote the sustainable management of these valuable river ecosystems.

REFERENCES

Andualem, T. G., Hewa, G. A., Myers, B. R., Peters, S., and Boland, J. (2023). Erosion and Sediment Transport Modeling: A Systematic Review. *Land*, 12(7), 1396.

Awal, R., Sapkota, P., Chitrakar, S., Thapa, B. S., Neopane, H. P., and Thapa, B. (2019). A general review on methods of sediment sampling and mineral content analysis. In *Journal of Physics: Conference Series*, 1266 (1), 012005). IOP Publishing.

Balouchi, B., Ruther, N., Mirzaahmadi, A., and Schwarzwälder, K. (2022). Two-dimensional (2D) depth-averaged numerical modeling of a braided river morphodynamics upstream of a dam reservoir. *Ele*, 283, 284.

Benn, D. I. and Owen, L. A. (2002). Himalayan glacial sedimentary environments A framework for reconstructing and dating the former extent of glaciers in high mountains. *Quat Int*, 97 (98).

Berry, W., Rubenstein, N., Melzion, B., and Hill., B. (2003). The biological effects of suspended and bedded sediment (SABS) in aquatic systems: a review. Internal Report of the U.S. Environmental Protection Agency, Office of Research and Development, Narragansett RI.

Boggs & Sam. (2006). *Principles of sedimentology and stratigraphy* (4th ed.). Upper Saddle River, N.J.: Pearson Prentice Hall.

Brunner, G.W. (2016). HEC-RAS River Analysis System User’s Manual; US Army Corps of Engineers: Davis, CA, USA.

Carson, M. A., and Griffiths, G. A. (1987). Influence of Channel Width on Bed Load Transport Capacity. *Journal of Hydraulic Engineering*, 113(12), 1489–1508.

Cassel, M., Lavé, J., Recking, A., Malavoi, J.-R., and Piégay, H. (2021). Bedload transport in rivers, size matters but so does shape. *Scientific Reports*, 11(1), 508.

Chiphang, N., Golom, T., Bandyopadhyay, A., and Bhadra, A. (2022). Modeling the impact of climate change on sediment yield from an Eastern Himalayan River Basin using ArcSWAT. *Arabian Journal of Geosciences*, 15(3), 232.

Choden, S. (n.d.). *Sediment Transport Studies in Punatsangchhu River, Bhutan*.

Coulibalya, L. K., and Coulibalyc, N. (2023). The impact of climate change on sediment transport capacity: a case study of the boubo coastal watershed. *Environment & Ecosystem Science (EES)*, 7(1), 01-12.

Czuba, J. A., and Foufoula-Georgiou, E. (2014). A network-based framework for identifying

Damgaard, J. S., Whitehouse, R. J. S., and Soulsby, R. L. (1997). Bed-Load Sediment Transport on Steep Longitudinal Slopes. *Journal of Hydraulic Engineering*, 123(12), 1130–1138.

da Silva, G. V., Strauss, D., Murray, T., Tomlinson, R., da Silva, A. P., Faivre, G., ... and Hemer, M. (2022). Impacts of climate change on Sediment Transport rates around Burleigh Heads. In Australasian Coasts & Ports 2021: Te Oranga Takutai, Adapt and Thrive: Te Oranga Takutai, Adapt and Thrive (pp. 985-

991). Christchurch, NZ: New Zealand Coastal Society..

Duba, C. (2016). *Reservoir Sedimentation Study for the Bunakha Hydro-electric Project* [Master thesis, NTNU].

Durafour, M., Jarno, A., Le Bot, S., Lafite, R., and Marin, F. (2015). Bedload transport for heterogeneous sediments. *Environmental Fluid Mechanics*, 15(4), 731–751.

Durafour, M., Jarno-Druaux, A., Marin, F., Lafite, R., Le Bot, S., and Blanpain, O. (2013, June 24). In-situ study of the influence of size and shape of sediments on bedload transport.

Estep, M. A., and Beschta, R. L. (1985). Transport of bedload sediment and channel morphology of a southeast Alaska stream. (PNW-RN-430; p. PNW-RN-430). U.S. Department of Agriculture, Forest Service, Pacific Northwest Forest and Range Experiment Station.

Favaro, E. A., and Lamoureux, S. F. (2015). Downstream patterns of suspended sediment transport in a High Arctic River influenced by permafrost disturbance and recent climate change. *Geomorphology*, 246, 359-369.

Fernandez, C., Wu, J. Q., McCool., D. K., and Stöckle., C. O. (2003). Estimating water erosion and sediment yield with GIS, RUSLE, and SEDD. *Journal of Soil and Water Conservation*, 58 (3), 128–136.

Galay, V. J. (1983). Causes of river bed degradation. *Water resources research*, *19* (5), 1057-1090.

Gomez, B., and Soar, P. J. (2022). Bedload transport: Beyond intractability. *Royal Society Open Science*, 9(3), 211932.

Hagg, W., Ram, S., Klaus, A., Aschauer, S., Babernits, S., Brand, D., Guggemoos, P., & Pappas, T. (2021). Hazard Assessment for a Glacier Lake Outburst Flood in the Mo Chu River Basin, Bhutan. *Applied Sciences*, *11*(20), 9463.

Hamzah, M. H. B. (2014). Study The 1d Quasi Jing Of Sediment Transport In Galing River By Using Hec-Ras (Doctoral dissertation, Universiti Malaysia Pahang).

Hassan, M., Chartrand, S., RadiĆ, V., Ferrer‐Boix, C., Buckrell, E., and McDowell, C. (2022). Experiments on the Sediment Transport along Pool‐Riffle Unit. *Water Resources* Research, 58.

Hou, L., Zhang, H., Li, L., Zhao, J., and Li, X. (2023). A Method for Calculating Water Demand for Sediment Transport Based on the Principles of River Dynamics. *Water*, 15(19), 3514.

Howard, A. D. (1998). Long profile development of bedrock channels: Interaction of weathering, mass wasting, bed erosion, and sediment transport. *Geophysical Monograph-American Geophysical Union*, 107, 297-319.

Hirsch, P. J., and Abrahams, A. D. (1981). The properties of bed sediments in pools and riffles. *Journal of Sedimentary Research*, 51(3), 757–760.

Jha, P. K., Vaithiyanathan, P., and Subramanian, K. (1993). Mineralogical characteristics of the sediments of a Himalayan River: Yamuna River a tributary of the Ganges. *Environ. Geol. Geol*., 22(1), 13 20.

Karim, M. F., & Kennedy, J. F. (1987). Velocity and sediment-concentration profiles in river flows. *Journal of Hydraulic Engineering*, 113(2), 159-176.

Koltermann, C. E., & Gorelick, S. M. (1996). Heterogeneity in sedimentary deposits: A review of structure‐imitating, process‐imitating, and descriptive approaches. *Water Resources Research*, *32*(9), 2617-2658

Korup, O. (2008). Rock type leaves topographic signature in landslide‐dominated mountain ranges. *Geophysical Research Letters*, 35.

KvoČka, D. (2021). One-dimensional sediment transport modelling with Engelund–Hansen and Ackers–White transport equations for the Lower Danube River. *Acta hydrotechnical*, 34(61), 103-117.

Ligong S, Sidek LM, Hayder G, Mohd Dom N. Application of Rainfall Threshold for Sediment-Related Disasters in Malaysia: Status, Issues and Challenges. *Water*. 2022; 14(20), 3212.

Mibei, G.K. (2014). Introduction to Types and Classification Of Rocks.

Mohammed, B. A., Sharfi, E. S. M., & Mordos, M. A. (2018). Simulation of River Bed Changes Upstream Merowe Dam. *University of Khartoum Engineering Journal*, 8(1).

Molinas, A., & Wu, B. (2001). Transport of sediment in large sand-bed rivers. *Journal of Hydraulic Research*, *39*(2), 135-146.

Montgomery, D. R., and Buffington, J. M. (1997). Channel-reach morphology in mountain drainage basins. *GSA Bulletin*, 109(5), 596–611.

Mossa, J., Chen, Y. H., Walls, S. P., Kondolf, G. M., and Wu, C. Y. (2017). Anthropogenic landforms and sediments from dredging and disposing sand along the Apalachicola River and its floodplain. *Geomorphology*, 294, 119-134.

Movahedinejad, S., Bohluly, A., Haghshenas, S. A., and Bidokhti, A. A. (2023). A 2D numerical model for simulation of cohesive sediment transport. *Computational Geosciences*, 1-13.

Nones, M., and Guo, Y. (2023). Can sediments play a role in river flood risk mapping? Learning from selected European examples. *Geo-environmental Disasters*, 10(1), 20.

Parker, G. (2007). Sedimentation Engineering." ASCE Manual 54, Chapter 3 (in press). Potential synchronizations and amplifications of sediment delivery in river basins. *Water Resources Research*, 50, 3826–3851.

Pradhan, P. M. S. (2004). *Improving sediment handling in the Himalayas*. OSH research, Nepal, 1-6.

Pitlick, J., & Cress, R. (2002). Downstream changes in the channel geometry of a large gravel bed river. Water resources research, 38(10), 34-1.

Weise, R. (2018). *1-Dimensional Hydraulic and Sediment Transport Modelling of an Emergency Spillway* (Doctoral dissertation, The University of Western Ontario (Canada).

Wright, L. D. (1977). Sediment transport and deposition at river mouths: a synthesis. *Geological Society of America Bulletin*, 88 (6), 857-868.

Young, W. J. (1989). Bedload transport in braided gravel-bed rivers: A hydraulic model study [*PhD Thesis*, Lincoln College, University of Canterbury].

Yusuf, A., Ojo, R., Idrees, M. O., Balogun, A. L., Salami, I. B., and Sani, O. S. (2023). Modelling flood hazards impacted by ungauged river in urbanised area using HEC-RAS and GIS. Nigerian Journal of Technological Development, 20(2), 83-92. *Nigerian Journal of Technological Development*. 20.

Yuan, S., Tang, H., Li, K., Xu, L., Xiao, Y., Gualtieri, C., and Melville, B. (2021). Hydrodynamics, sediment transport and morphological features at the confluence between the Yangtze River and the Poyang Lake. *Water Resources Research*, 57(3), e2020WR028284.

Zarifsanayei, A. R., Etemad-Shahidi, A., Cartwright, N., and Strauss, D. (2020). Long-term prediction of longshore sediment transport in the context of climate change. *Coastal Engineering Proceedings*, (36v), 15-15.

Zhang, J., Zhang, X., Li, R., Chen, L., & Lin, P. (2017). Did streamflow or suspended sediment concentration changes reduce sediment load in the middle reaches of the Yellow River?. *Journal of Hydrology*, 546, 357-369.

Zhang, T., Li, D., East, A. E., Walling, D. E., Lane, S., Overeem, I., and Lu, X. (2022). Warming-driven erosion and sediment transport in cold regions. *Nature Reviews Earth & Environment*, 3(12), 832-851.